

protonation constants (which are nonexistent in the thia ether systems) and upon electrostatic interactions of the positively charged Cu(II) with charged ligands (also absent in the current systems). The apparent absence of significant adducts with $\text{Cu}(\text{H}_2\text{O})_6^{2+}$ and $\text{Cu}([\text{15}] \text{aneS}_2)^{2+}$ in this study indicates that this phenomenon is not universal. However, future investigators might be well advised to check out the possibility of such adduct formation when equilibrium data are analyzed.

Conclusions

1. The conditional stability constants (K_{CuL}') for the Cu(II)-tetrathia ether complexes appear to increase by approximately 20-fold when the perchlorate ion concentration is increased from 0.01 to 1.0 M. This effect is independent of the cation, but qualitatively similar results are obtained in the presence of BF_4^- or CF_3SO_3^- .

2. The increase in the conditional stability constants is attributed to the formation of a perchlorate adduct, CuLX^+ , for which the formation constant, K_{1X}° , appears to exhibit a value of approximately 20 M^{-1} for each Cu(II)-tetrathia ether complex studied. The K_{1X}° values may be somewhat in error due to errors in activity coefficient calculations, the presence of significant side reactions with Cu^{2+} (which were ignored in our analysis), or contributions from the K_{2X} term in eq 22. Nonetheless, the

evidence suggests that interactions between the perchlorate ion and the Cu(II)-tetrathia ether complexes do exist and that the perchlorate is most probably associated within the inner-coordination sphere of the Cu(II) ion.

3. The corrected values for the Cu(II)-tetrathia ether complex stability constants (K_{CuL}°) extrapolated to zero perchlorate ion concentration are approximately 80% as large as the conditional stability constant values determined experimentally in the presence of 0.010 M ClO_4^- or 50–60% of the conditional values determined at 0.10 M ClO_4^- .

4. The evidence suggesting the coexistence of two forms of copper(II) complex in solution containing perchlorate ion (i.e., CuL^{2+} and CuLX^+) implies that the physical parameters measured for these systems, such as equilibrium constants and reaction rate constants, are composite values that cannot be directly interpreted. The resolution of meaningful constants, including thermodynamic functions and activation parameters, can only be achieved by studying these systems under conditions of varying perchlorate ion concentration.

Acknowledgment. This work was supported, in part, by the National Institute of General Medical Sciences under Grant GM-20424.

Registry No. ClO_4^- , 14797-73-0.

Contribution from the Research Laboratory for Nuclear Reactors, Tokyo Institute of Technology, O-okayama, Meguro-ku, Tokyo 152, Japan

Kinetics and Mechanism of the Substitution of Dibenzoylmethanate for Acetylacetonate in $\text{UO}_2(\text{acac})_2\text{L}$ (L = Dimethyl Sulfoxide, *N,N*-Dimethylformamide, and Trimethyl Phosphate)

Woo-Sik Jung, Hiroshi Tomiyasu, and Hiroshi Fukutomi*

Received January 2, 1986

Kinetics of the substitution of dibenzoylmethanate (dbm) for one acetylacetonate in $\text{UO}_2(\text{acac})_2\text{L}$ (acac = acetylacetonate; L = Me_2SO (dimethyl sulfoxide), dmf (*N,N*-dimethylformamide), and tmp (trimethyl phosphate)) have been studied in solvents L by spectrophotometry. Under the conditions $[\text{UO}_2(\text{acac})_2\text{L}] \gg [\text{Hdbm}]$, the rate law for the substitution reactions is expressed as rate = $k_2K[\text{UO}_2(\text{acac})_2\text{L}][\text{Hdbm}]/(1 + K[\text{UO}_2(\text{acac})_2\text{L}])$, where $K = [\text{UO}_2(\text{acac})_2\text{dbmH}]/[\text{UO}_2(\text{acac})_2\text{L}][\text{Hdbm}]$. The equilibrium constant K decreases as the basicity of ligand L increases. Rate constant k_2 corresponds to that of proton transfer from coordinated Hdbm to leaving acac in $\text{UO}_2(\text{acac})_2\text{dbmH}$, which is evidenced by the deuterium isotope effect on the rate and the linearity of the plot of $\log k_2$ vs. the reciprocal dielectric constant. The rate of the k_2 path is accelerated in amphiprotic solvents. Rate constants (s^{-1}) at 25 °C and activation parameters ΔH^\ddagger (kJ mol^{-1}) and ΔS^\ddagger ($\text{J K}^{-1} \text{mol}^{-1}$) for the k_2 path are 11.6×10^{-3} , 31.3 ± 1.0 , and -177 ± 4 for $\text{UO}_2(\text{acac})_2\text{dmf}$ and 2.31×10^{-3} , 50.2 ± 0.4 , and -127 ± 14 for $\text{UO}_2(\text{acac})_2\text{tmp}$. These results are discussed in connection with those of the acac-exchange reactions in $\text{UO}_2(\text{acac})_2\text{L}$ and $\text{Th}(\text{acac})_4$.

Kinetics of exchange reactions between metal chelate complexes of various β -diketonates (HB) and free ligands have been studied by the NMR line-broadening method,¹⁻⁹ isotopic labeling method with ^{14}C ,¹⁰⁻¹² and spectrophotometric method.¹³ Although rates

of the exchange reactions differ greatly with central metal ions, mechanisms so far proposed are classified into three types according to the rate-determining step: (1) breaking of one of the metal-oxygen bonds;¹¹ (2) formation of an intermediate containing a dangling unidentate ligand (B^-) and an incoming ligand (HB in the enol form);⁹⁻¹² (3) intramolecular proton transfer from coordinated HB to leaving B^- .³⁻⁷ In previous papers^{1,2} we reported the kinetic study of exchange reactions of acac in $\text{UO}_2(\text{acac})_2\text{L}$ (acac = acetylacetonate; L = dimethyl sulfoxide (Me_2SO), *N,N*-dimethylformamide (dmf)) in *o*-dichlorobenzene and proposed the mechanism of type 1.

In this paper we report the kinetic results of substitution reactions of dibenzoylmethanate (dbm) for one acac in $\text{UO}_2(\text{acac})_2\text{L}$

- (1) Ikeda, Y.; Tomiyasu, H.; Fukutomi, H. *Inorg. Chem.* **1984**, *23*, 3197.
- (2) Ikeda, Y.; Fukutomi, H. *Inorg. Chim. Acta* **1986**, *115*, 223.
- (3) Fujiwara, N.; Tomiyasu, H.; Fukutomi, H. *Bull. Chem. Soc. Jpn.* **1984**, *57*, 1576.
- (4) Fujiwara, N.; Tomiyasu, H.; Fukutomi, H. *Bull. Chem. Soc. Jpn.* **1985**, *58*, 1386.
- (5) Folcher, G.; Keller, N.; Kiener, C.; Paris, J. *Can. J. Chem.* **1977**, *55*, 3559.
- (6) Tanner, G. M.; Tuck, D. G.; Wells, E. J. *Can. J. Chem.* **1972**, *50*, 3950.
- (7) Khvostik, G. M.; Sokolov, V. N.; Grebenschikov, G. K.; Toropov, S. A.; Kondratenkov, G. P. *Sov. J. Coord. Chem. (Engl. Transl.)* **1979**, *5*, 534.
- (8) Nixon, A. J. C.; Eaton, D. R. *Can. J. Chem.* **1978**, *56*, 1012.
- (9) Adams, A. C.; Larsen, E. M. *Inorg. Chem.* **1966**, *5*, 814.

- (10) Watanabe, A.; Kido, H.; Saito, K. *Inorg. Chem.* **1981**, *20*, 1107.
- (11) Kido, H. *Bull. Chem. Soc. Jpn.* **1980**, *53*, 82.
- (12) Nishizawa, M.; Saito, K. *Bull. Chem. Soc. Jpn.* **1978**, *51*, 483.
- (13) Sekine, T.; Inaba, K. *Bull. Chem. Soc. Jpn.* **1984**, *57*, 3083.

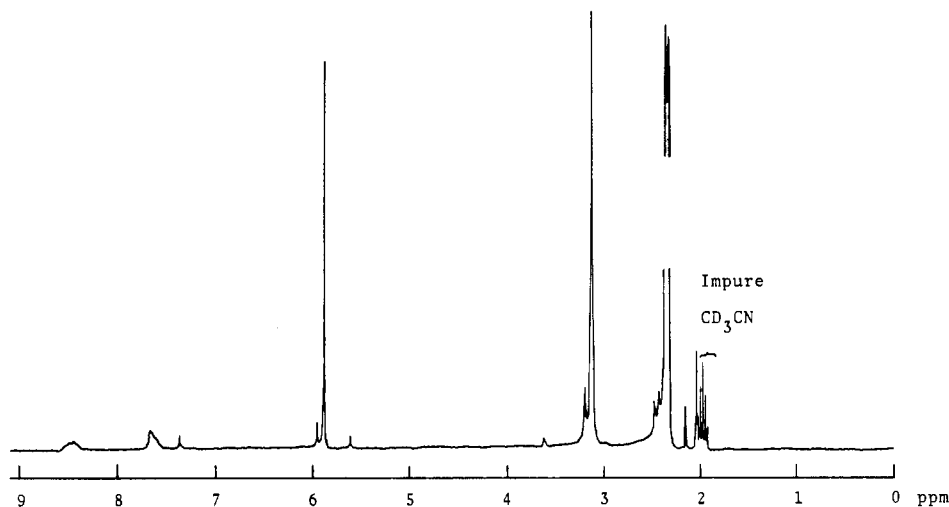
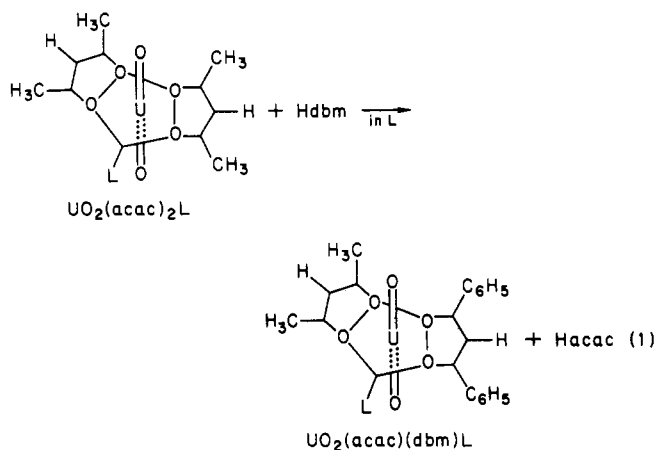


Figure 1. ^1H NMR spectrum after dissolution of $\text{UO}_2(\text{acac})_2\text{Me}_2\text{SO}$ (2.15×10^{-2} M) and Hdbm (2.63×10^{-3} M) in CD_3CN at -34°C .

(L = Me_2SO , dmf, and trimethyl phosphate (tmp)) in solvents L



and the results of kinetic isotope effects, where deuterated dibenzoylmethane (Ddbm) was used, for a further understanding of exchange mechanisms of β -diketonate in $\text{UO}_2(\beta\text{-diketonate})_2\text{L}$ complexes.

Experimental Section

Materials. The complexes $\text{UO}_2(\text{acac})_2\text{Me}_2\text{SO}$, $\text{UO}_2(\text{acac})_2\text{dmf}$, $\text{UO}_2(\text{acac})_2\text{tmp}$, and $\text{UO}_2(\text{dbm})_2\text{Me}_2\text{SO}$ were synthesized by the same method as described in previous papers.^{14,15} Anal. Calcd for $\text{UO}_2(\text{acac})_2\text{tmp}$: C, 25.67; H, 4.14. Found: C, 25.69; H, 3.83. Dibenzoylmethane was recrystallized from methanol and dried under vacuum. Deuterated dibenzoylmethane (Ddbm)¹⁶ was prepared by dissolving Hdbm in a boiling solution of acetone and D_2O (4:1) as described in the literature.¹⁷ The fraction of deuteration was determined by ^1H NMR measurements.¹⁶ Dimethyl sulfoxide, *N,N*-dimethylformamide, trimethyl phosphate, butyronitrile, and *o*-dichlorobenzene were distilled under reduced pressure, and nitromethane, 1,2-dichloroethane, and chloroform were distilled before use. Acetonitrile- d_3 (CD_3CN) was dried over 4A molecular sieves.

- (14) Ikeda, Y.; Tomiyasu, H.; Fukutomi, H. *Bull. Chem. Soc. Jpn.* **1983**, *56*, 1060.
 (15) Ikeda, Y.; Tomiyasu, H.; Fukutomi, H. *Bull. Chem. Soc. Jpn.* **1984**, *57*, 2925.
 (16) Incomplete deuterium incorporation results in formation of four isotopomers of Hdbm, i.e. $\text{H}_5\text{C}_6\text{CO}(\text{OH})\text{CHCOC}_6\text{H}_5$, $\text{H}_5\text{C}_6\text{CO}(\text{OH})\text{CDCOC}_6\text{H}_5$, $\text{H}_5\text{C}_6\text{CO}(\text{OD})\text{CHCOC}_6\text{H}_5$, and $\text{H}_5\text{C}_6\text{CO}(\text{OD})\text{CDCOC}_6\text{H}_5$. In the present paper, the latter two isotopomers are referred to as Ddbm and the others Hdbm. The fraction of deuterium incorporation was determined by relative intensities of ^1H NMR signals of benzene-ring protons (S_b) and hydroxyl proton (S_h), where the fraction is given by $(0.1S_b - S_h)/0.1S_b$.
 (17) Tayyari, S. F.; Zeegers-Huyskens, T.; Wood, J. L. *Spectrochim. Acta, Part A* **1979**, *35A*, 1265.

Table I. Chemical Shifts (ppm, Me_4Si Reference) of ^1H Resonances of a Solution after Dissolving $\text{UO}_2(\text{acac})_2\text{Me}_2\text{SO}$ (2.15×10^{-2} M) and Hdbm (2.63×10^{-3} M) in CD_3CN at -34°C

compd	acac/Hacac			dbm	
	CH_3-	$=\text{CH}-$	$-\text{CH}_2-$	C_6H_5-	$=\text{CH}-$
$\text{UO}_2(\text{acac})_2\text{Me}_2\text{SO}$	2.33	5.91		ca. 7.7	7.35
	2.36			ca. 8.5	
$\text{UO}_2(\text{acac})(\text{dbm})\text{Me}_2\text{SO}$	2.43	5.99		ca. 7.7	7.42
	2.47			ca. 8.5	
Hacac (enol) ^a	2.03	5.64			
Hacac (keto) ^a	2.14		3.62		

^a Free Hacac in the enol or keto form.

Measurements of ^1H NMR and UV-Visible Spectra. ^1H NMR spectra were measured by using a JEOL JNM-FX 100 FT-NMR spectrometer equipped with a JNM-VT-3B temperature controller. Measurements of UV-visible spectra were carried out on a JASCO UVI-DEC-505 spectrophotometer with thermostated cell compartments ($\pm 0.2^\circ\text{C}$) and 1-cm quartz cells. Molar extinction coefficients ($\text{M}^{-1}\text{cm}^{-1}$, $\text{M} = \text{mol dm}^{-3}$) determined at 450 nm and 25°C are as follows: 314 ± 5 for $\text{UO}_2(\text{acac})_2\text{Me}_2\text{SO}$, 309 ± 1 for $\text{UO}_2(\text{acac})_2\text{dmf}$, 4111 ± 48 for $\text{UO}_2(\text{dbm})_2\text{Me}_2\text{SO}$, and 3888 ± 43 for $\text{UO}_2(\text{dbm})_2\text{dmf}$.

Kinetic Measurements. Pseudo-first-order conditions ($[\text{UO}_2(\text{acac})_2\text{L}] \gg [\text{Hdbm}]$) were used throughout the study of reactions expressed by eq 1. The rate of the substitution reactions of one coordinated acac in $\text{UO}_2(\text{acac})_2\text{L}$ was given by $2k_{\text{obsd}}[\text{Hdbm}]_{\text{enol}}$, which is approximately equal to $2k_{\text{obsd}}[\text{Hdbm}]$ because Hdbm exists almost entirely in the enol form.¹⁸ The pseudo-first-order rate constants k_{obsd} were determined from plots of $\ln(A_\infty - A_t)$ vs. time, where A_t and A_∞ are absorbances at times t and infinity, respectively, at the wavelength 450 nm. Kinetic experiments were performed at least twice.

Results

Stoichiometry of Substitution Reactions. In order to confirm the stoichiometry of substitution reactions (eq 1), ^1H NMR spectra were measured under the same conditions as in kinetic measurements. An example of the spectra is illustrated in Figure 1, where the measurement was performed for a solution containing $\text{UO}_2(\text{acac})_2\text{Me}_2\text{SO}$ and Hdbm in CD_3CN . Assignments of signals are given in Table I. No signals of free Hdbm were observed, which indicates that the reaction proceeded almost up to 100%. It is to be noted that ^1H resonances of coordinated ligands in $\text{UO}_2(\text{acac})(\text{dbm})\text{Me}_2\text{SO}$ occur at lower field than those in $\text{UO}_2(\text{acac})_2\text{Me}_2\text{SO}$ and that doublet signals of methyl protons of acac in these complexes are due to intramolecular exchange reactions.¹⁹ Molar extinction coefficients of reaction products at 450 nm were determined at 25°C on the assumption that the substitution reactions are complete. The values are found to be 2205 ± 41 and $2029 \pm 81 \text{ M}^{-1}\text{cm}^{-1}$ for $\text{UO}_2(\text{acac})(\text{dbm})\text{Me}_2\text{SO}$ and $\text{UO}_2(\text{acac})(\text{dbm})\text{dmf}$, respectively, and both values are ap-

(18) Allen, G.; Dwek, R. A. *J. Chem. Soc. B* **1966**, 161.

(19) Ikeda, Y.; Tomiyasu, H.; Fukutomi, H. *Inorg. Chem.* **1984**, *23*, 1356.

Table II. Kinetic Data for the Substitution of dbm for acac in $\text{UO}_2(\text{acac})_2\text{L}$ in L (L = Me_2SO and tmp)

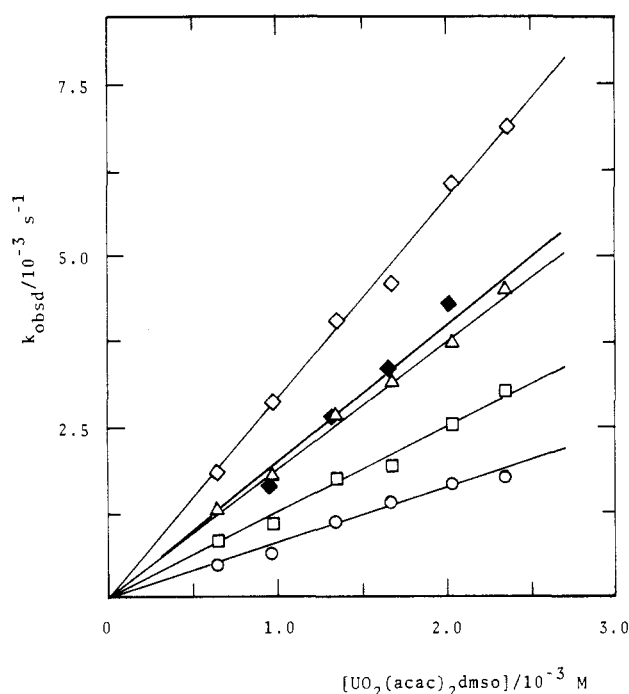
L	param	rate constant				$\Delta H^\ddagger / \text{kJ mol}^{-1}$	$\Delta S^\ddagger / \text{J K}^{-1} \text{mol}^{-1}$
		20 °C	24 °C	28 °C	32 °C		
Me_2SO	p or $k_2K^a/\text{M}^{-1} \text{s}^{-1}$	0.794 ± 0.061	1.28 ± 0.08	1.84 ± 0.07	2.93 ± 0.12 (2.09 ± 0.13) ^b	77.0 ± 2.8	16.4 ± 9.6
tmp	$k_2^c/10^{-3} \text{s}^{-1}$	1.49 ± 0.13	2.12 ± 0.24	2.85 ± 0.15	3.47 ± 0.21	50.2 ± 0.4	-127 ± 14
	$k_2^d/10^{-3} \text{s}^{-1}$	4.39 (25 °C)				63.4 ± 5.8	-77.4 ± 19.6

^a $k_2K(25^\circ\text{C}) = 1.44 \text{ M}^{-1} \text{ s}^{-1}$. ^b By Ddbm (46%). ^c $k_2(25^\circ\text{C}) = 2.31 \times 10^{-3} \text{ s}^{-1}$. ^d In 1:1 (v/v) tmp–nitromethane mixed solvent.

Table III. Kinetic Data for the Substitution of dbm for acac in $\text{UO}_2(\text{acac})_2\text{dmf}$ in dmf

temp/°C	q/s	$r/10^{-1} \text{ M s}$	q^{-1} or $k_2^a/10^{-3} \text{ s}^{-1}$	(q/r) or K^b/M^{-1}
12	157 ± 39.0	8.14 ± 0.44	6.39 ± 2.11	193 ± 56
16	126 ± 27.2	4.16 ± 0.30	7.91 ± 2.17	303 ± 95
20	133 ± 9.40	2.00 ± 0.10	7.51 ± 0.57	666 ± 32
24	88.2 ± 4.20	1.16 ± 0.05	11.4 ± 0.8	762 ± 70

^a $k_2(25^\circ\text{C}) = 11.6 \times 10^{-3} \text{ s}^{-1}$, $\Delta H^\ddagger = 31.3 \pm 1.0 \text{ kJ mol}^{-1}$, $\Delta S^\ddagger = -177 \pm 4 \text{ J K}^{-1} \text{ mol}^{-1}$. ^b $\Delta H = 81.1 \pm 1.7 \text{ kJ mol}^{-1}$, $\Delta S = 328 \pm 6 \text{ J K}^{-1} \text{ mol}^{-1}$.

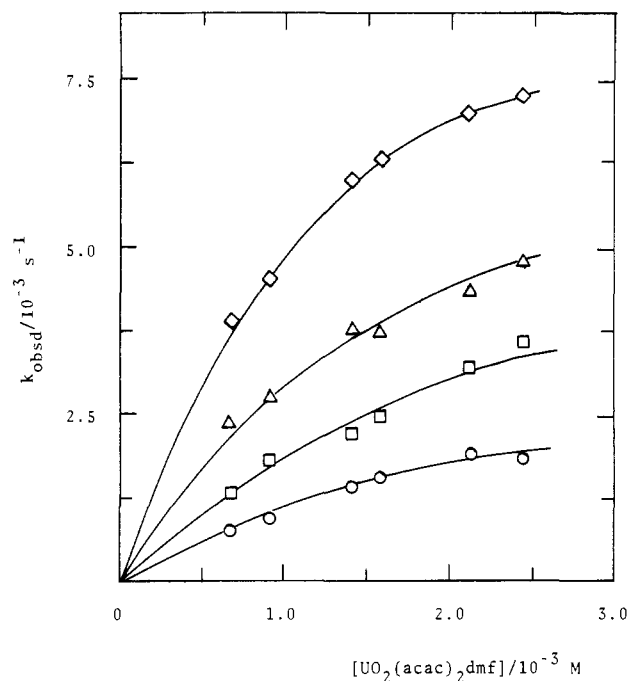
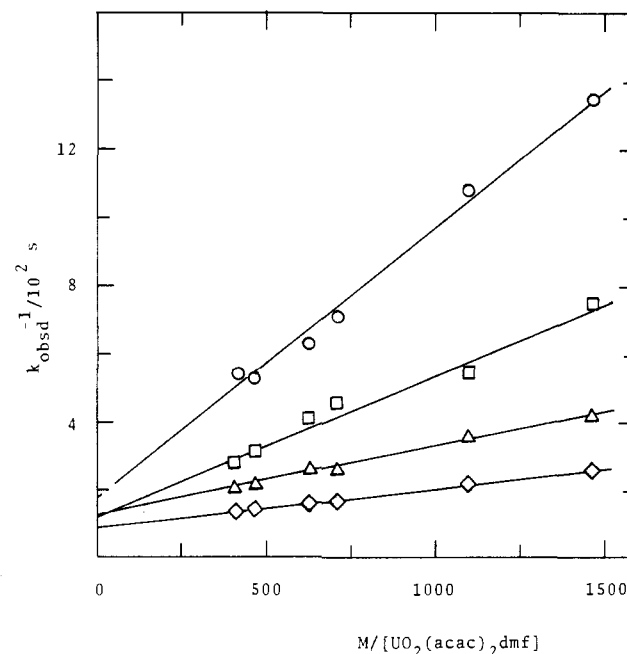
**Figure 2.** Plots of k_{obsd} vs. $[\text{UO}_2(\text{acac})_2\text{Me}_2\text{SO}]$ for the substitution of dbm for acac in $\text{UO}_2(\text{acac})_2\text{Me}_2\text{SO}$: (O) 20 °C; (□) 24 °C; (Δ) 28 °C; (◇) 32 °C; (◆) 32 °C, by Ddbm (46%).

proximately the mean of those for $\text{UO}_2(\text{acac})_2\text{L}$ and $\text{UO}_2(\text{dbm})_2\text{L}$ (L = Me_2SO and dmf; Experimental Section). It is evident from the above results that the reaction products are only $\text{UO}_2(\text{acac})(\text{dbm})\text{L}$ and Hacac and that any reaction other than a substitution reaction (eq 1) does not occur under the conditions studied.

Substitution Reactions in Solvents L. The dependence of the pseudo-first-order rate constants (k_{obsd}) on $[\text{UO}_2(\text{acac})_2\text{Me}_2\text{SO}]$ is shown in Figure 2, where the rate constants vary linearly with $[\text{UO}_2(\text{acac})_2\text{Me}_2\text{SO}]$; i.e. $k_{\text{obsd}} = p[\text{UO}_2(\text{acac})_2\text{Me}_2\text{SO}]$. The values of p obtained from the slopes in Figure 2 are listed in Table II. It is noted that the rate of the substitution at 32 °C when Ddbm is used (46%) is 1.4 times slower than that by Hdbm. For the $\text{UO}_2(\text{acac})_2\text{dmf}$ complex, on the other hand, k_{obsd} depends on $[\text{UO}_2(\text{acac})_2\text{dmf}]$ in its low region but tends to approach limiting values in its high region (Figure 3). Plots of $1/k_{\text{obsd}}$ against $1/[\text{UO}_2(\text{acac})_2\text{dmf}]$ give straight lines with intercepts as shown in Figure 4 and yield the expression

$$1/k_{\text{obsd}} = q + r/[\text{UO}_2(\text{acac})_2\text{dmf}] \quad (2)$$

The values of q and r obtained from Figure 4 are given in Table

**Figure 3.** Plots of k_{obsd} vs. $[\text{UO}_2(\text{acac})_2\text{dmf}]$ for the substitution of dbm for acac in $\text{UO}_2(\text{acac})_2\text{dmf}$: (O) 12 °C; (□) 16 °C; (Δ) 20 °C; (◇) 24 °C.**Figure 4.** Plots of $1/k_{\text{obsd}}$ vs. $1/[\text{UO}_2(\text{acac})_2\text{dmf}]$ for the substitution of dbm for acac in $\text{UO}_2(\text{acac})_2\text{dmf}$: (O) 12 °C; (□) 16 °C; (Δ) 20 °C; (◇) 24 °C.

III. Figure 5 shows that k_{obsd} for $\text{UO}_2(\text{acac})_2\text{tmp}$ is independent of the complex concentration. The k_{obsd} value at each temperature is given in Table II. The rate for $\text{UO}_2(\text{acac})_2\text{tmp}$ in a mixture (1:1, v/v) of nitromethane and tmp was also measured, and the result is shown in Table II.

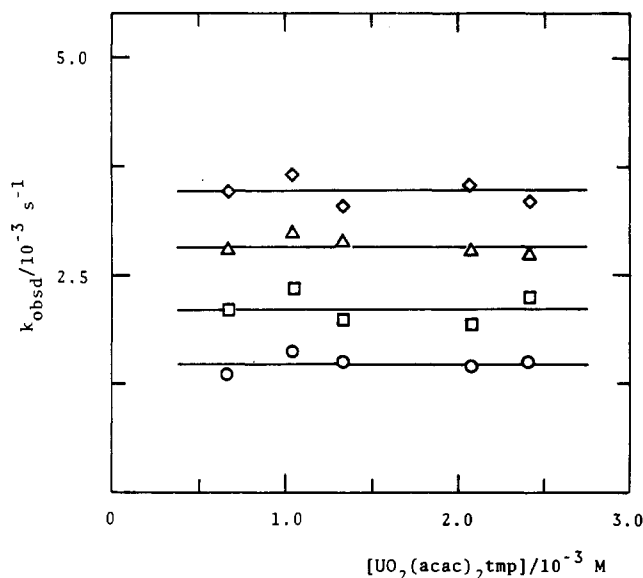


Figure 5. Plots of k_{obsd} vs. $[\text{UO}_2(\text{acac})_2\text{tmp}]$ for the substitution of dbm for acac in $\text{UO}_2(\text{acac})_2\text{tmp}$: (O) 20 °C; (□) 24 °C; (Δ) 28 °C; (◇) 32 °C.

Table IV. Rate Constants (25 °C) of the Substitution of dbm for acac in $\text{UO}_2(\text{acac})_2\text{tmp}$ in 1:1 (v/v) Mixed Solvents with tmp and Their Dielectric Constants

solvent	$k_2/10^{-3} \text{ s}^{-1}$	ϵ^a
dmf ^b	11.6	36.7
nitromethane (nm)	4.39	28
tmp ^c	2.31	20.6 ^d
butyronitrile (bn)	2.67	21
1,2-dichloroethane (dce)	2.18	16
<i>o</i> -dichlorobenzene (dcb)	1.38	15
chloroform	ca. 20	13

^a It is assumed that the dielectric constant of mixed solvent is equal to $(\epsilon_{\text{tmp},25^\circ\text{C}} + \epsilon_{\text{solvent},25^\circ\text{C}})/2$: Decroocq, D. *Bull. Soc. Chim. Fr.* **1964**, 127. ^b For $\text{UO}_2(\text{acac})_2\text{dmf}$ in neat dmf solvent. ^c Neat solvent. ^d At 20 °C.

Rate in Various Solvents and Influence of H_2O . Solvent effects on the rate for $\text{UO}_2(\text{acac})_2\text{tmp}$ were studied in 1:1 (v/v) mixed solvents with tmp, and the results are summarized in Table IV. In the mixture (1:1, v/v) with amphiprotic solvents such as methanol and 1-propanol, the rates were so fast that the rate constants were not obtained spectrophotometrically. The k_{obsd} value increased linearly on addition of H_2O (<0.3 M) to $\text{UO}_2(\text{acac})_2\text{tmp}$ solution in tmp (Figure 6) and was given by

$$k_{\text{obsd}} = k_2 + k_c[\text{H}_2\text{O}] \quad (3)$$

where $k_2 = (3.39 \pm 0.10) \times 10^{-3} \text{ s}^{-1}$ and $k_c = (7.75 \pm 0.62) \times 10^{-3} \text{ M}^{-1} \text{ s}^{-1}$ at 32 °C. The former value is in agreement with the k_{obsd} value at 32 °C for $\text{UO}_2(\text{acac})_2\text{tmp}$ in neat tmp solvent within experimental errors (Table II).

Discussion

The results in this study showed that k_{obsd} is highly dependent on L. This might be well explained by the mechanism given in Figure 7. The reaction is initiated by the substitution of Hdbm in the enol form for L in $\text{UO}_2(\text{acac})_2\text{L}$, the rate of which is expected to be very fast,^{14,15} followed by the proton-transfer process (k_2 path) from the coordinated Hdbm to one of two acac in intermediate II. A complex similar to II, $\text{UO}_2(\text{acac})_2\text{acacH}$, has been reported,²⁰ where Hacac or Hdbm is coordinated as a unidentate ligand, and both complexes have the same pentagonal-bipyramidal structure as $\text{UO}_2(\text{acac})_2\text{H}_2\text{O}$.^{21,22} If the rate-

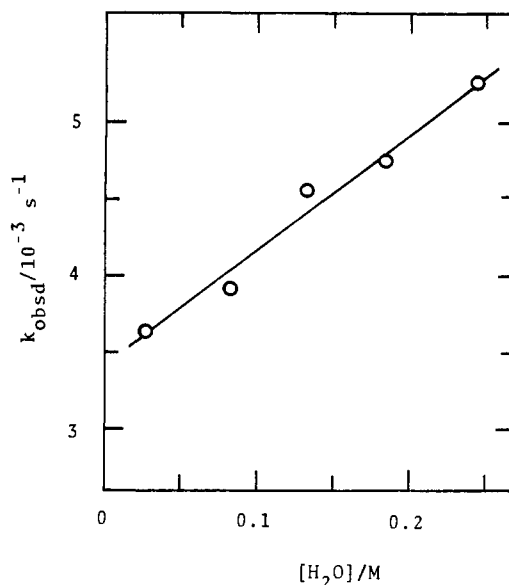


Figure 6. Plot of k_{obsd} vs. $[\text{H}_2\text{O}]$ for the effect of added H_2O on the substitution of dbm for acac in $\text{UO}_2(\text{acac})_2\text{tmp}$ at 32 °C.

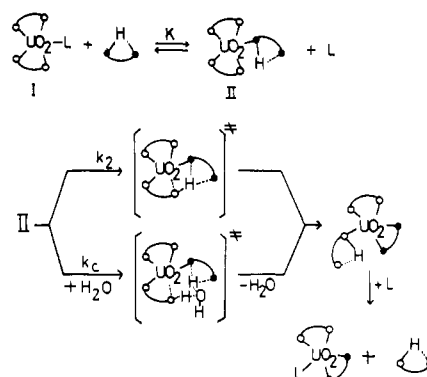


Figure 7. Possible mechanism of the substitution of dbm for acac in $\text{UO}_2(\text{acac})_2\text{L}$ in the presence and in the absence of H_2O . HO \bullet and H \bullet represent Hacac and Hdbm in the enol form, respectively.

determining step is the k_2 path in the absence of H_2O , then k_{obsd} is given by

$$k_{\text{obsd}} = \frac{k_2 K[\text{I}]}{1 + K[\text{I}]} \quad (4a)$$

$$\frac{1}{k_{\text{obsd}}} = \frac{1}{k_2} + \frac{1}{k_2 K} \frac{1}{[\text{I}]} \quad (4b)$$

It is expected that the equilibrium constant K decreases as the basicity of ligand L increases. Since the basicities of L decrease in the order Me_2SO , dmf, and tmp,^{23,24} the corresponding equilibrium constants are assumed to increase in that order.

In the limiting case $K[\text{I}] \ll 1$, k_{obsd} becomes $k_2 K[\text{I}]$ from eq 4a. This is the case with $\text{UO}_2(\text{acac})_2\text{Me}_2\text{SO}$, and $p = k_2 K$. If $K[\text{I}] \gg 1$, eq 4a can be simplified as $k_{\text{obsd}} = k_2$ and the rate becomes independent of $[\text{I}]$ as is seen in Figure 5 for $\text{UO}_2(\text{acac})_2\text{tmp}$. This leads to the conclusion that k_{obsd} in the $\text{UO}_2(\text{acac})_2\text{tmp}$ system corresponds to the rate constant for the k_2 path. Equation 4b is consistent with eq 2 for $\text{UO}_2(\text{acac})_2\text{dmf}$. The parameters k_2 and K , therefore, correspond to q^{-1} and q/r , respectively. The values of k_2 and K for $\text{UO}_2(\text{acac})_2\text{dmf}$ obtained from values q and r are listed in Table III.

If the k_2 path is the proton-transfer process from dipolar Hdbm to negatively charged acac in $\text{UO}_2(\text{acac})_2\text{dbmH}$, we may expect

(20) Comys, A. E.; Gatehouse, B. M.; Wait, E. *J. Chem. Soc.* **1958**, 4655.
 (21) Frasson, E.; Bombieri, G.; Panattoni, C. *Nature (London)* **1964**, 202, 1325.
 (22) Haigh, J. M.; Thornton, D. A. *Inorg. Nucl. Chem. Lett.* **1970**, 6, 231.

(23) Jung, W.-S.; Tomiyasu, H.; Fukutomi, H. *Bull. Chem. Soc. Jpn.* **1985**, 58, 938.
 (24) Gutmann, V. *Coordination Chemistry in Nonaqueous Solutions*; Springer-Verlag: Berlin, 1968.

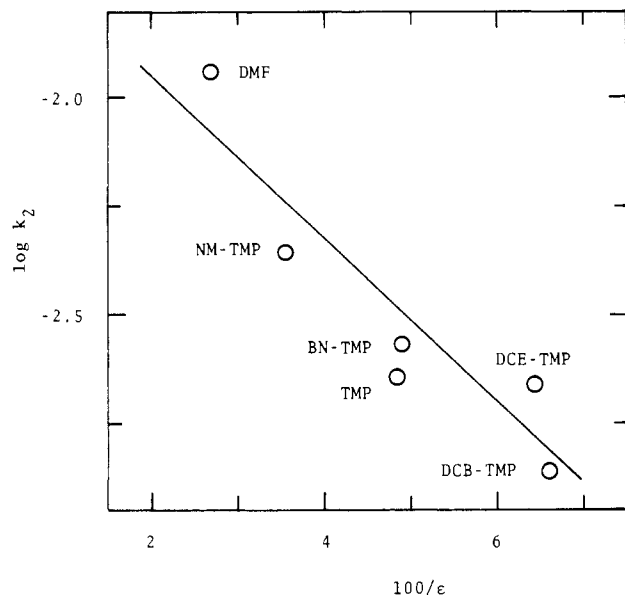


Figure 8. Plot of $\log k_2$ against the reciprocal dielectric constant for the solvent effect on the substitution of dbm for acac in $\text{UO}_2(\text{acac})_2\text{L}$ at 25 °C. Solvent abbreviations: dmf = *N,N*-dimethylformamide; nm = nitromethane; tmp = trimethyl phosphate; bn = butyronitrile; dce = 1,2-dichloroethane; dcb = *o*-dichlorobenzene.

solvent effects on the rate. The dependence of the rate constant on the dielectric constant of a medium was treated by Amis²⁵ using a Coulomb energy approach for the ion-dipole interaction. A consideration of mutual potential energy between an ion of charge Z_A and a dipole of dipole moment μ_B in the distance r_{AB} leads to

$$\log k = \log k_\infty + \frac{Z_A e \mu_B}{2.303 k_B T \epsilon r_{AB}^2} \quad (5)$$

where k_∞ is the rate constant in a medium with the dielectric constant of infinite magnitude, k_B is the Boltzmann constant, T is the absolute temperature, and ϵ represents the dielectric constant of the medium. Since k_{obsd} is equal to k_2 for $\text{UO}_2(\text{acac})_2\text{tmp}$, solvent effects on the rate were studied for the complex. Figure 8 shows the dependence of $\log k_2$ on $1/\epsilon$, and a linear relationship with a negative slope supports the k_2 path involving the interaction between a negatively charged ion and a dipole. The rate constants for the k_2 path of $\text{UO}_2(\text{acac})_2\text{Me}_2\text{SO}$ in Me_2SO can be estimated from conditions that $K[\text{I}] \ll 1$ and $k_2 K$ is $1.44 \text{ M}^{-1} \text{ s}^{-1}$ at 25 °C (Table II). The fact that the estimated k_2 value is above 0.02 s^{-1} at 25 °C appears to be reasonable if one considers the high dielectric constant (46.7 at 25 °C) of Me_2SO .

The acceleration of the rate by addition of H_2O (Figure 6) may be attributed to the fact that there is an additional k_c path where H_2O acts as a proton donor and acceptor through hydrogen bonding with intermediate II (Figure 7). Consequently, the rate constant for the k_2 path in the presence of H_2O is given by $k_2 + k_c[\text{H}_2\text{O}]$ as written in eq 3, where the rate constant k_2 corresponds to that for the k_2 path in the absence of H_2O . In the previous paper,³ we reported that the acac exchange in $\text{Th}(\text{acac})_4$ proceeded through the mechanism of type 3 and found that the reaction was retarded by the addition of H_2O , where the retardation arose from the competition between H_2O and incoming Hacac in the enol form at the ninth coordination site. However, the retardation effect by addition of H_2O may be lessened by the acceleration effect due to the above-mentioned k_c path in the proton-transfer process.

In a similar way amphiprotic solvents, e.g. alcohols, can accelerate the rate in the k_2 path, though the k_c values for alcohols are supposed to be smaller than that for H_2O . The k_c path is considered to be responsible for the fact that the rate constant

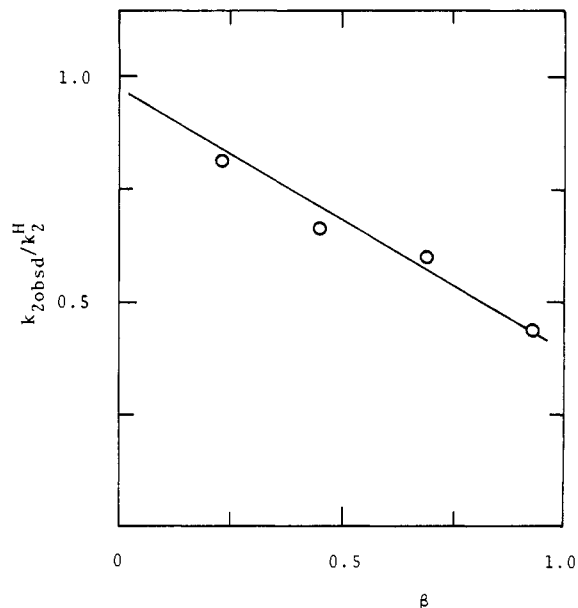


Figure 9. Plot of $k_{2,\text{obsd}}/k_2^{\text{H}}$ against the fraction of deuteration for the substitution of dbm for acac in $\text{UO}_2(\text{acac})_2\text{tmp}$ at 32 °C.

(ca. 0.02 s^{-1} at 25 °C) in the CHCl_3 -tmp mixed solvent (Table IV) is too large in view of the low dielectric constant of CHCl_3 . It is noted that the rate of acac exchange in $\text{Th}(\text{acac})_4$ is faster in CDCl_3 than in CD_3CN .³

In order to investigate the k_2 path in more detail, the deuterium isotope effect on the rate was studied by using Ddbm. The kinetic isotope effect ($\alpha = k_2^{\text{H}}/k_2^{\text{D}}$) in the k_2 path is given by²⁶

$$k_{2,\text{obsd}}/k_2^{\text{H}} = 1 - (1 - 1/\alpha)\beta \quad (6)$$

where $k_{2,\text{obsd}}$ is the observed rate constant for the k_2 path when the fraction of deuteration is β ¹⁶ and k_2^{H} and k_2^{D} are rate constants for $\beta = 0$ and $\beta = 1$, respectively. Rate measurements were carried out for $\text{UO}_2(\text{acac})_2\text{tmp}$ in tmp with varying β . As is expected from eq 6, the plot of $k_{2,\text{obsd}}/k_2^{\text{H}}$ vs. β gives a straight line with an intercept of approximately unity (0.97 ± 0.03) (Figure 9). The value of α was determined to be 2.35 ± 0.35 from the slope in Figure 9. For $\text{UO}_2(\text{acac})_2\text{Me}_2\text{SO}$ the substitution rate was 1.4 times slower with Ddbm (46%) than Hdbm (Figure 2). Assuming that the isotope effect on K is negligible, α becomes 2.6 for $\text{UO}_2(\text{acac})_2\text{Me}_2\text{SO}$, which is in satisfactory agreement with that for $\text{UO}_2(\text{acac})_2\text{tmp}$ within experimental errors. The deuterium isotope effect suggests that the rate-determining step involves the proton-transfer process. The kinetic isotope effect in this study is larger than that in the mechanism of type 2^{10,11} but smaller than that (ca. 9)²⁷ in the acac exchange in $\text{Th}(\text{acac})_4$. The latter may be partially explained by the fact that the smaller the difference in pK between HX and HY (i.e. the more symmetric the transition state), the larger the kinetic isotope effect for the proton-transfer reaction between X^- and HY or Y^- and HX.²⁸ The pK value (13.25) of Hdbm is larger than that (12.70) of Hacac in the enol form.²⁹

It was proposed in previous papers^{1,2} that acac-exchange reactions in $\text{UO}_2(\text{acac})_2\text{L}$ ($\text{L} = \text{Me}_2\text{SO}$ and dmf) proceeded through a mechanism where breaking of one of the metal-oxygen bonds is the rate-determining step. However, these exchange reactions seem to be explained also by the mechanism proposed in this study (Figure 7). In other words, the reactions are initiated by the substitution of Hacac in the enol form for L in $\text{UO}_2(\text{acac})_2\text{L}$, where the equilibrium constant is considered to be smaller than

(25) Amis, E. S. *Solvent Effects on Reaction Rates and Mechanisms*; Academic: New York, London, 1966.

(26) It was assumed that the kinetic isotope effect is only due to the difference between -OH and -OD and that the secondary isotope effect by deuteration of =CH- is negligible.

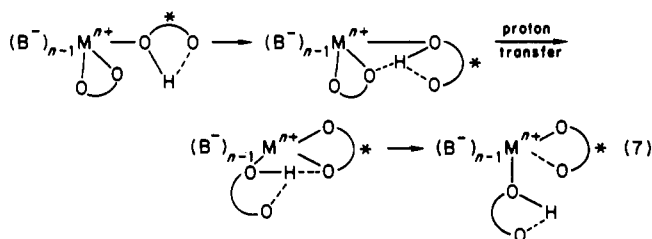
(27) Fujiwara, N. Ph.D. Dissertation, Tokyo Institute of Technology, 1983.

(28) Bell, R. P. *The Proton in Chemistry*; Chapman and Hall: London, 1973; Chapter 12.

(29) Lintvedt, R. L.; Holtzclaw, H. F., Jr. *Inorg. Chem.* 1966, 5, 239.

those of the present study. The retardation effect by addition of free base L can be interpreted by the decrease in concentration of $\text{UO}_2(\text{acac})_2\text{acacH}$ with the addition of L. This interpretation is similar to that of the retardation in acac exchange in $\text{Th}(\text{acac})_4$ but different from that in the exchange of acac in $\text{VO}(\text{acac})_2$,¹² where the retardation is attributed to the formation of an outer-sphere intermediate with the added base.

As mentioned above, the present substitution reaction in $\text{UO}_2(\text{acac})_2\text{L}$ and the exchange reaction of acac in $\text{Th}(\text{acac})_4$ proceed through the type 3 mechanism, where the rate-determining step is the proton-transfer process. Although there is a similarity between the mechanisms of both systems, the reaction rates differ considerably from each other. The difference in rates of the proton-transfer processes can be understood by assuming that the process consists of three steps:



where M^{n+} is a metal ion and $\text{HO}^{\ominus}\text{O}$ represents a β -diketonate (HB) in the enol form. In the first step in eq 7, incoming HB^* and coordinated B^- come near each other to make a hydrogen bridge between HB^* and B^- . The second step is the proton transfer

including the formation of the hydrogen bridge. The third step is the breaking of the hydrogen bridge between coordinated B^- and leaving HB. The difference in rates is mainly attributed to the difference in ΔG^\ddagger values for the first step, since the variation in ΔG^\ddagger values for the proton-transfer step is expected to be relatively small. The unidentate β -diketonate as a proton donor, which was coordinated to the metal ion with a large ionic radius, rotates about a metal-oxygen bond so freely that the β -diketonate can easily orientate so as to favor proton transfer. Large negative ΔS^\ddagger values (Tables II and III) seem to reflect the steric hindrance in the first step. Consequently, the difference in rates between $\text{UO}_2(\text{acac})_2\text{L}$ and $\text{Th}(\text{acac})_4$ or $\text{U}(\text{acac})_4$ ⁷ is explained by the difference in ionic radii of central metal ions. The steric hindrance may be responsible in part for the difference in rates of exchange between $\text{Th}(\text{acac})_4$ and $\text{Th}(\text{tta})_4$ ⁴ (tta = 2-thionyltrifluoroacetate) because tta is more bulky than acac.

Although many studies on the intermolecular proton-transfer reaction have been reported, data on the rate of the intramolecular proton-transfer reaction, particularly in organic solvents, are not available. More detailed studies on the $\text{UO}_2(\beta$ -diketonate)₂L system are in progress in order to elucidate the steric hindrance and kinetic isotope effect in the intramolecular proton-transfer process, and information on these aspects is to be considered in a future report.

Acknowledgment. W.-S.J. wishes to thank Dr. Y. Ikeda for providing uranyl complexes.

Registry No. $\text{UO}_2(\text{acac})_2(\text{Me}_2\text{SO})$, 71357-22-7; $\text{UO}_2(\text{acac})_2(\text{dmf})$, 89145-11-9; $\text{UO}_2(\text{acac})_2(\text{tmp})$, 102575-53-1; dbm, 19274-26-1; D_2 , 7782-39-0.

Contribution from the Lash Miller Chemical Laboratories, University of Toronto, Toronto, Ontario, Canada M5S 1A1

Reactions of Transition-Metal Atoms with Arenes, Arene-Functionalized Alkanes, Oligo(ethylene oxides), and Polysiloxanes. 4

Mark P. Andrews[†] and Geoffrey A. Ozin*

Received October 18, 1985

New synthetic, chemical, and spectroscopic (optical, Raman, IR, EPR) experiments aimed at further elucidation of the details of the near-room-temperature reactions of metal atoms with arene-functionalized liquid polysiloxanes to produce organometallic polymers and polymer-supported metal clusters are described. By examining the reactions of V, Cr, and Mo atoms with model arenes, arene-functionalized alkanes, and arene-functionalized oligo(ethylene oxides), one is able to gain insight into the role of arene substituents, bis(arene)metal cross-links, and the solvating backbone in the mode of formation and stabilization of metal cluster sites on the polysiloxane. The chemical and physical homogeneity of the resulting polymers is also assessed.

Introduction

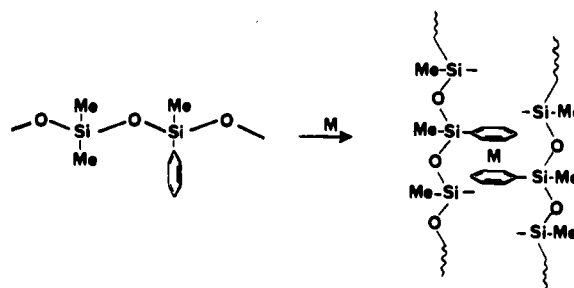
A theme running through much of our recent metal atom research has been to find ways of generating and stabilizing metal clusters at or close to room temperature in various fluid trapping media and to devise methods for investigating their physical and chemical properties within the trapping medium itself.¹ The ability to transfer the metal aggregates from the fluid intact to supports such as carbon, inorganic oxides, and zeolites emerged as a result of such investigations.^{1,2}

In this paper we focus attention on a method of metal cluster formation in the liquid phase that is based on the direct sequential addition of metal atoms according to sequence 1 during the metal



atom deposition process. This reaction is viewed as occurring at a site preformed in the support medium, which invariably contains arene functionalities, usually linked to oligoalkanes, oligo(ethylene oxides), and oligo- and polysiloxanes. In particular, the arene substituents inhibit competing metal atom polymerization reactions

Scheme I



by chemically trapping the atomic diffusant. In general, these liquid supports permit chemical reactions of metal atoms with ligands to occur at higher temperatures, which will result in a more favorable competitive balance between bis(arene)M complex

- (1) Ozin, G. A. *CHEMTECH* 1985, 15, 488 and references cited therein.
- (2) Ozin, G. A.; Andrews, M. P. U.S. Patent 454 886, 1982. Ozin, G. A.; Hugues, F.; Nazar, L. F. U.S. Patent 454 886, 1982. Nazar, L. F.; Ozin, G. A.; Hugues, F.; Godber, J.; Rancourt, D. *J. Mol. Catal.* 1983, 21, 313. Ozin, G. A.; Andrews, M. P. *Stud. Surf. Sci. Catal.*, in press.

[†]Current address: AT&T Bell Laboratories, Murray Hill, NJ 07974.